POLITECNICO DI TORINO
Repository ISTITUZIONALE

Distinguishing short circuit and normal operation currents in DC urban light railway systems

(Article begins on next page)

19 April 2024

Distinguishing Short Circuit and Normal Operation Currents in DC Urban Light Railway Systems

E. Pons*, , P. Colella*, , R. Rizzoli† and R. Tommasini‡,
*Politecnico di Torino - Dipartimento Energia
Torino, 10129, ITALY
Email: enrico.pons@polito.it
†Infratrasporti.To Srl
Torino, 10122, ITALY
Email: Roberto.Rizzoli@infrato.it
‡Prof. Tommasini passed away on January 20th, 2017

Abstract—**DC urban light railway systems are used as public transportation systems in many towns worldwide. In these systems, short circuit currents are often similar, both in steady state magnitude and in rate-of-rise, to normal operation currents. In order to properly set the protection relays, to obtain short circuit discrimination and to avoid nuisance trippings, it is important to analyse short circuit and normal operation current patterns. This paper presents the results of measurement campaigns performed for this purpose on the tram network of Turin, in Northern Italy.**

I. Introduction

Light railway systems are used as public transportation systems in many towns worldwide. For these systems the DC supply is widely used, at different voltage levels [1].

For these DC tram networks, the Traction Electrification System (TES) is normally fed by power substations, which contain the power transformers, AC/DC converters, protective relays and circuit breakers; from these substations several DC feeders (positive cables) are used to energize the Overhead Contact System (OCS). The return current is collected by the rails and by the negative cables [2].

Different types of faults can happen in DC tram networks. Some faults, as close-in bolted faults (short circuits between positive and negative conductors, inside the substation or in its vicinity) give rise to very high short circuit currents, characterized by a high rate-of-rise di/dt in the first instants and by a high steady state magnitude. These types of fault are easily recognized by overcurrent protections and extra-rapid circuit breakers trip. Some faults, instead, like arcing faults (e.g. ground faults along the line) or distant bolted faults produce smaller steady state values and rate-of-rises and are difficult to detect: both the steady state fault current magnitude and the initial rate-of-rise are in fact comparable to normal operation currents parameters [3].

For these reasons, standard protective relays, such as instantaneous and time-delayed over-current protections, are not sufficient; also the rate-of-rise protection of modern relays is quite difficult to be properly set, in order to obtain short-circuit discrimination and to avoid nuisance tripping.

The application guide EN 50123-7-1 (Measurement, control and protection devices for specific use in d.c. traction systems) specifies that, in particular in light-rail systems with overhead contact lines, special attention should be paid to the requirements for protection against indirect contacts. The rate-of-rise relay would satisfy this need, but the application guide itself reports that the setting is not always easy and recommends field trials to show that it will trip for the most distant fault condition [4].

In case the fault is not recognized by protective relays, the workers can be subject to risk of electric shock inside the feeding substations and people along the tram lines. Dangerous voltages can in fact be present on the rails and on extraneous conductive parts inside the substation when fault currents are circulating [2].

In previous works the authors studied ground faults inside the substation and along the line, developing appropriate steady state models for the different elements which constitute the TES [2], [5]. The results of these studies show that there are conditions in which dangerous voltages can be present on accessible metallic parts but standard over-current protections do not recognize the fault.

A first possibility that can be exploited in order to improve short circuit discrimination is to use rate-of-rise over-current protections. In [3] the optimization of the protection settings is presented. It used real operation recordings in a representative feeder for the settings improvement based on empirical data.

Nevertheless, as previously mentioned, also the simple rate-of-rise protection can be difficult to be properly set. In fact, besides tram acceleration di/dt, much higher current derivatives can be observed when a vehicle crosses the boundary between two different zones of the OCS. The contact system, in fact, is normally divided in zones, fed by different feeders and protected by different circuit breakers. In tram networks, usually, the different zones are separated by a short insulating section or by a short element in which the two conductors run parallel to each other. In railways instead, normally, the commutation between two zones is guaranteed by a 40-50 m long section, where the power supply to the trains is provided

at the same time by both contact wires, insulated each other, that run parallel at about 40 cm distance. In all of these cases, with small differences associated to the different geometry of the commutation system, when the vehicle pantograph leaves completely the old zone, high current gradients are observed. This phenomenon is very well explained, for railway systems, in [6].

More sophisticated protection systems use a combination of current gradient di/dt, current increment ΔI and delay duration ΔT for short circuit discrimination [1]. In any case, in order to properly set these protection systems, a good knowledge of normal operation and short circuit currents patterns is required.

In this paper the results of measurements campaigns are presented. The measurements were performed on the tram network of Turin, in Northern Italy, in order to study the current patterns in normal operation and in case of short circuit, for the proper setting of the protection systems.

The rest of the paper is organized in this way: section II presents the results of short circuit tests; section III presents the results of a measurement campaign on tram acceleration currents; section IV presents the current patterns for the zone commutation phenomenon; in section V the different patterns are compared and the results are discussed. Finally, some conclusions are given.

II. SHORT CIRCUIT CURRENTS

Short circuit currents in DC systems fed by rectifiers can be, for our purposes, approximated to an exponential with an overshoot that depends mainly on the DC side impedance [7]–[9]. For the cases we are mostly interested in, i.e. arcing faults or distant bolted faults, the DC side impedance is high and the overshoot is not present. The relevant parameters that must be kept into account are:

- the steady-state current magnitude I_0;
- the initial rate-of-rise of the current $\dfrac{di_0}{dt}$.

In the traction system where the measurement campaigns have been carried out, the AC/DC converters are constituted by 12-pulse rectifiers. Therefore the relevant values can be calculated (with some approximations, due for example to impedance variation during the fault [10]) as presented in eq. 1 and eq. 2 [7]:

$$I_0 = \frac{2 \cdot U_{d0}}{\sqrt{3} \cdot \sqrt{(R_{AC} + R_{DC})^2 + \omega^2 \cdot L_{AC}^2}} \tag{1}$$

$$\frac{di_0}{dt} = \frac{U_{d0}}{L_{AC} + L_{DC}} \tag{2}$$

where:

- U_{d0} is the rectifier no load voltage;
- R_{AC} is the AC side resistance, which is mainly constituted by the transformer windings resistances;
- R_{DC} is the DC side resistance, which is mainly constituted by the resistance of feeder cables, OCS, rails and return conductors;
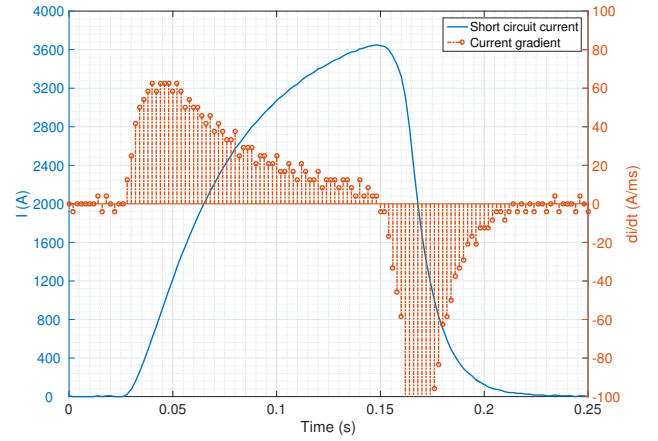- ω is the AC system frequency;

Fig. 1. Short circuit current for distant bolted fault.

- L_{AC} is the AC side inductance, which is mainly constituted by the transformer windings inductances;
- L_{DC} is DC side inductance.

Different measurement campaigns have been performed in order to study real short circuit currents. Test short circuits have been performed both in the substations and along the lines, with or without a series additional resistance to limit the short circuit current magnitude.

The measurements have been performed with a high speed digital recorder. The voltage drop on a shunt resistance was measured.

An example of the recorded waveform for a bolted fault far from the feeding substation is presented in Fig. 1. In the same figure the rate-of-rise is also reported. In this case the extra-rapid circuit breaker in the substation tripped, and so the short circuit current could not reach its steady state value I_0.

The equations presented (eq. 1 and eq. 2) can be useful to determine the approximate line parameters from real measurements and to extend the measurement results for faults in different positions along the line or with different series impedance.

In Fig. 2 and Fig. 3 the cumulative distribution functions (cdf) of the current increment and current rate-of-rise are reported, respectively, for short circuit currents recorded during the measurements campaign. The cdf for the experimental data in a vector X is defined as the probability that X will take a value less than or equal to x. Fig. 2 and Fig. 3 show therefore the probability that a short circuit will have a ΔI or a di/dt lower than a certain threshold.

The variation range for these two important parameters, for short circuit currents, is rather wide, in fact, $20\ A/ms \leq di/dt \leq 800\ A/ms$ and $500\ A \leq \Delta I \leq 14500\ A$.

III. TRAM ACCELERATION CURRENTS

Tram acceleration currents have stochastic patterns that depend on the road traffic conditions and on the driver operations. Typical acceleration currents however are related
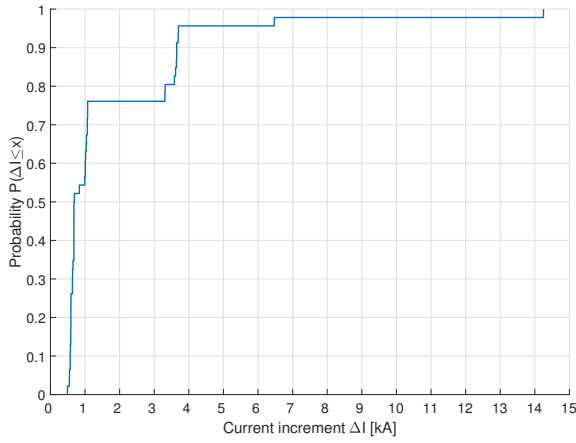
Fig. 2. Cumulative distribution function (cdf) of current increment for short circuit currents.
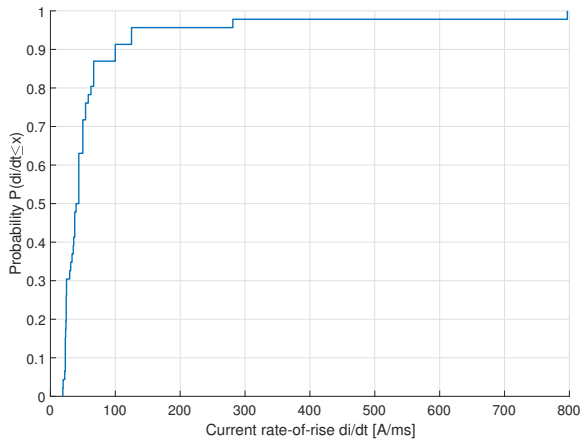

Fig. 4. Tram acceleration currents - old variable speed drive with rheostatic control.

Fig. 3. Cumulative distribution function (cdf) of current rate-of-rise for short circuit currents.
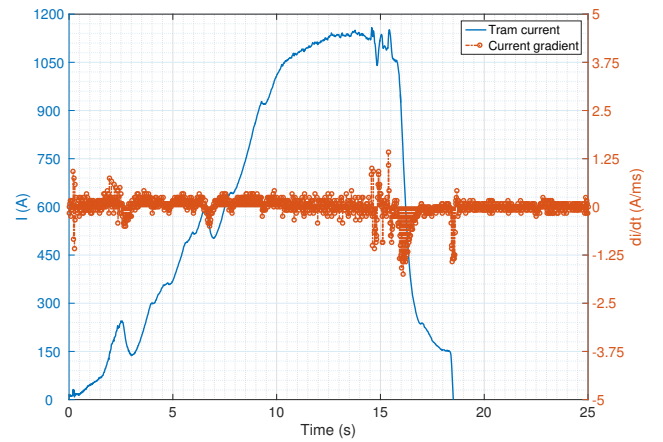
Fig. 5. Tram acceleration currents - modern variable frequency drive.

to the type of drive adopted by the vehicles. In Fig. 4 the typical current profile absorbed by an old vehicle equipped with DC motors and rheostatic control is presented. Vice-versa, in Fig. 5, the typical current profile of a modern vehicle with induction motors and variable frequency drives is showed. Also in this case the measurements have been carried out using a high speed digital recorder. It was located inside a power substation and connected to the shunt resistance on the feeder of the zone where the vehicles under test were circulating. Typical gradients are in the range from 1 A/ms to 5 A/ms.

In Fig. 6 and Fig. 7 the complementary cumulative distribution functions (ccdf) of the current increment and current rate-of-rise are reported, respectively, for tram acceleration currents, including all types of vehicles that can circulate in the tram network in Turin. The ccdf shows how often the random variable is above a particular level, so, in this case, the probability that a tram acceleration current will have a ΔI or a di/dt higher than a certain threshold.
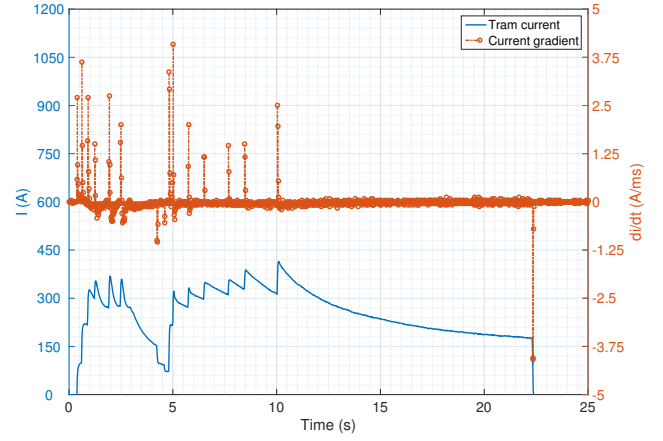
In this case, the variation range for the two parameters is much smaller, as $0.2\ A/ms \leq di/dt \leq 4.3\ A/ms$ and $10\ A \leq \Delta I \leq 650\ A$.

IV. ZONE COMMUTATION CURRENTS

As previously mentioned, besides tram acceleration di/dt and ΔI, much higher current derivatives and increments can be observed when a vehicle crosses the boundary between two different zones of the OCS. In Fig. 8, as an example, the current absorbed when a modern vehicle equipped with induction motors and variable frequency drives enters the new zone is presented.

By comparing the gradients presented in Fig. 1 for the short circuit and Fig. 8 for the zone commutation, it is immediately evident that comparable values of rate-of-rise can be reached, in this example close to 80 A/ms.

Other types of vehicles produce different current patterns when they cross the boundary between two different zones of the OCS.
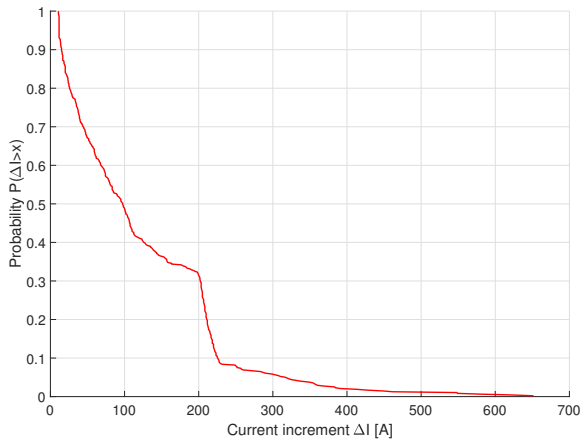
Fig. 6. Cumulative distribution function (cdf) of current increment for tram acceleration currents.
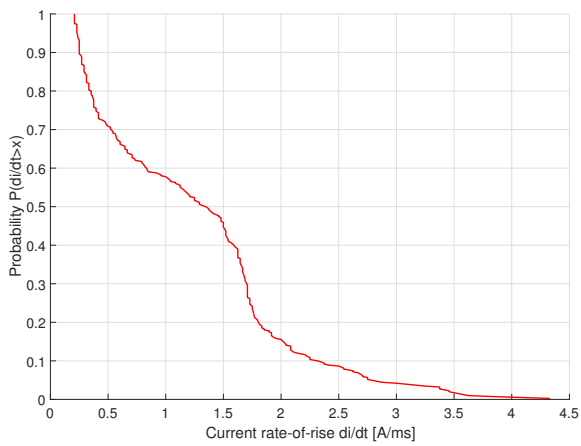

Fig. 7. Cumulative distribution function (cdf) of current rate-of-rise for tram acceleration currents.
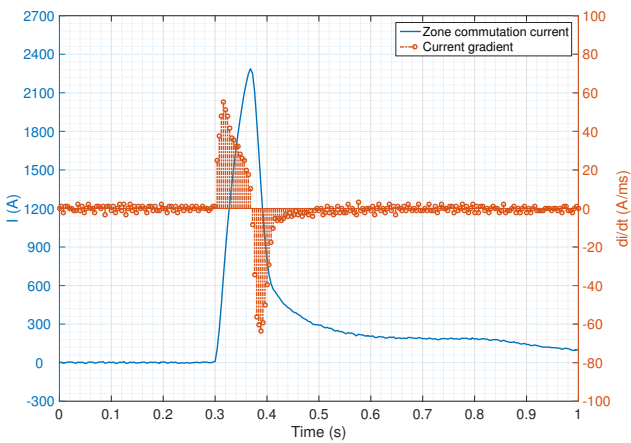

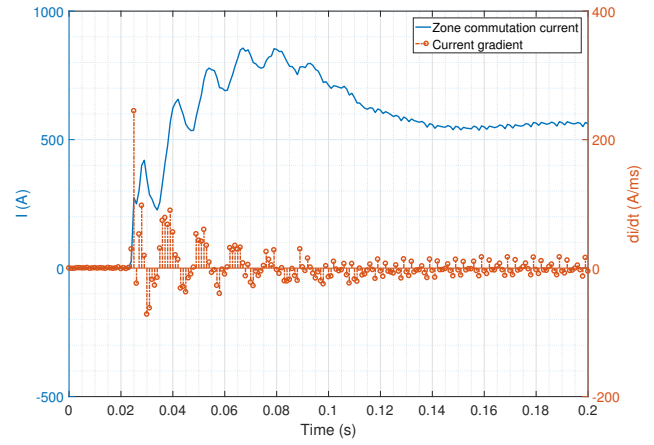Fig. 8. Zone commutation current - vehicle with variable frequency drive.

Fig. 9. Zone commutation current - vehicle with chopper (A).
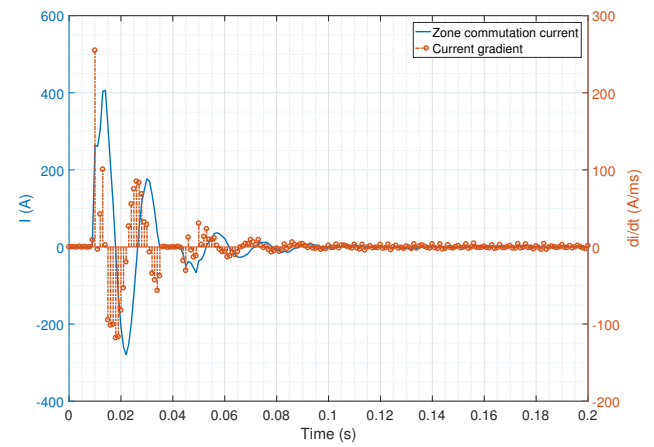

Fig. 10. Zone commutation current - vehicle with chopper (B).

In Fig. 9 and Fig. 10 two additional examples are presented. They are both recorded when a vehicle equipped with a chopper speed controller crosses the boundary between two zones. In the first case, the vehicle speed is high, the time required to cross the insulating element is low, and the electronics does not reset. In the second case, vice versa, the vehicle speed is low, the time required to cross the insulating element is high, and the electronics resets.

In both cases very high current rates-of rise are recorded. The interesting point, however, is that the current starts decreasing after a short period of time, lower than 0.1 s.

For these cases, the measurements have been carried out installing the high speed digital recorder on board of the vehicle and positioning a current clamp on the vehicle imperial, where the power cables receive the current from the pantograph.

In Fig. 11 and Fig. 12 the complementary cumulative distribution functions of the current increment and current rate-of-rise are reported, respectively, for zone commutation currents.

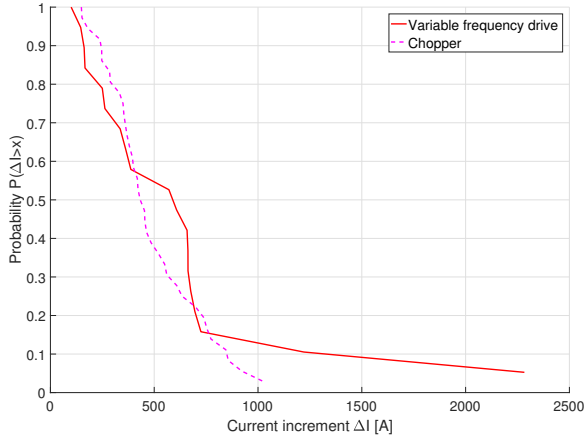In both figures the ccdf for vehicles equipped with variable

Fig. 11. Cumulative distribution function (cdf) of current increment for zone commutation currents.
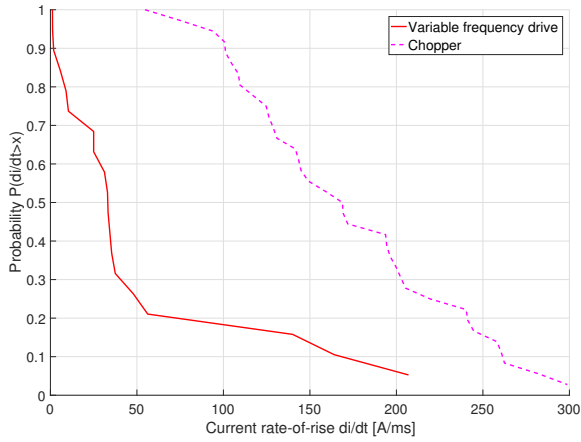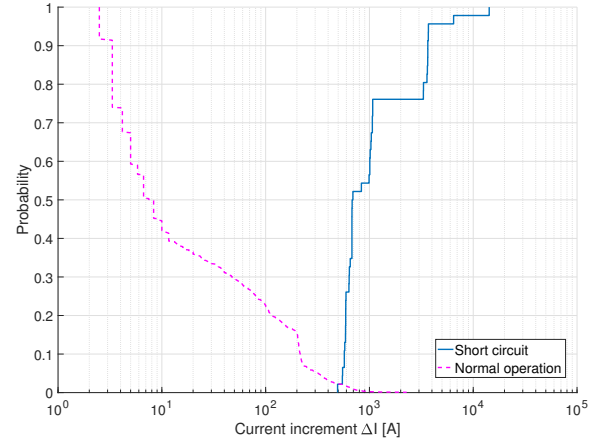

Fig. 13. Cumulative distribution function (cdf) of current increment comparison.

Fig. 12. Cumulative distribution function (cdf) of current rate-of-rise for zone commutation currents.
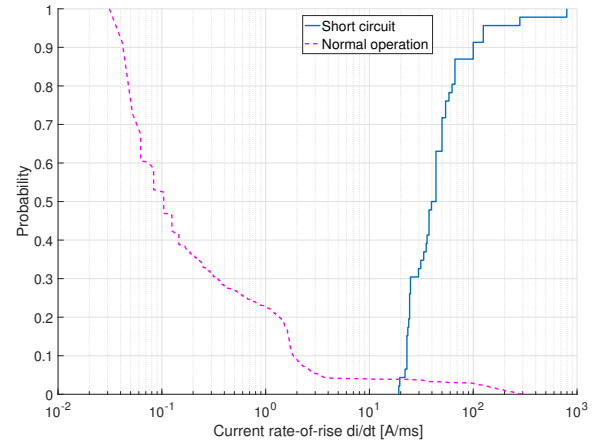
Fig. 14. Cumulative distribution function (cdf) of current rate-of-rise comparison.

frequency drive and chopper are compared. It can be observed that variable frequency drives can generate much higher current increments ΔI, but lower current rates-of-rise di/dt.

In the case of zone commutation currents it is particularly interesting to analyze the variation range of the two parameters, as this can be compared with the variation range for short circuit currents.

For zone commutation currents the variation range is again quite large, as $1\ A/ms \leq di/dt \leq 300\ A/ms$ and $100\ A \leq \Delta I \leq 2300\ A$.

V. Discussion

Once the current patterns, for the different possible cases related to normal operation and short circuit, have been individually studied, it is interesting to make a comprehensive analysis. For this purpose the current patterns have been grouped in normal currents (including acceleration and zone commutation currents) and short circuit currents. An overall ccdf has been calculated for normal operation currents, that

can be compared, in the same plot, with the cdf of short circuit currents. In Fig. 13 the comparison is performed for the current increment ΔI, while in Fig. 14 for the rate-of-rise di/dt. A logarithmic scale is used for current increment and rate-of-rise to improve comprehension, because the variation ranges are different.

The presented plots show that there is a range of values clearly related to fault conditions and a range of values clearly related to normal operations. However, there is also a range of values, for both ΔI and di/dt, in which fault conditions and normal operation are overlapped.

The setting of the protection relays, in terms of current increment and rate-of-rise, should be a compromise between fault discrimination and nuisance tripping.

Plots similar to those presented in Fig. 13 and Fig. 14 could be therefore used to evaluate, for a certain proposed setting of the relay, the probability of having nuisance tripping and the probability of missing the detection of certain fault events

characterized by a high impedance.

The plots presented in this paper in Fig. 13 and Fig. 14 can provide only qualitative indications and not accurate information on the probabilities. In fact, they have been constructed by putting together all the data acquired during the measurement campaigns, but the number of available measurements for the different vehicle types, for acceleration and zone commutation currents and for short circuit tests were not the same.

VI. CONCLUSION

The problem of short circuit discrimination in DC urban light railway systems is studied in this paper. In order to optimize the protection settings, several measurements campaigns have been performed. In particular, currents related to tram acceleration, zone commutation and short circuits have been considered. The results of the campaigns have been presented and discussed, also resorting to a statistical analysis and to the presentation of cumulative distribution functions and complementary distribution functions.

The results show that there is a range of values clearly related to fault conditions and a range of values clearly related to normal operations. However, there is also a range of values, for both current increment and rate-of-rise, in which fault conditions and normal operation are overlapped.

For this reason the setting of the protection relays should be a compromise between fault discrimination and nuisance tripping.

A good opportunity can be provided by the time delay setting, as zone commutation currents start to decrease after a very short time, while short circuit currents last till the protection trips.

REFERENCES

[1] M. Li, J. He, Z. Bo, H. Yip, L. Yu, and A. Klimek, "Simulation and algorithm development of protection scheme in dc traction system," in *PowerTech, 2009 IEEE Bucharest*. IEEE, 2009, pp. 1–6.

[2] E. Pons, R. Tommasini, and P. Colella, "Electrical safety of dc urban rail traction systems," in *Environment and Electrical Engineering (EEEIC), 2016 IEEE 16th International Conference on*. IEEE, 2016, pp. 1–6.

[3] M. Reis, "Optimization of dc feeder rate of rise overcurrent protection settings using delta i cumulative distribution," in *Industrial and Commercial Power Systems Technical Conference, 2004 IEEE*. IEEE, 2004, pp. 63–66.

[4] *Railway applications - Fixed installations - D.C. switchgear Part 7-1: Measurement, control and protection devices for specific use in d.c. traction systems - Application guide*. Standard EN 50123-7-1, 2003.

[5] E. Pons, R. Tommasini, and P. Colella, "Fault current detection and dangerous voltages in dc urban rail traction systems," *IEEE Transactions on Industry Applications*, Accepted for publication.

[6] E. Cinieri, A. Fumi, V. Salvatori, and C. Spalvieri, "A new high-speed digital relay protection of the 3-kvdc electric railway lines," *Power Delivery, IEEE Transactions on*, vol. 22, no. 4, pp. 2262–2270, 2007.

[7] C. Pires, S. Nabeta, and J. R. Cardoso, "Second-order model for remote and close-up short-circuit faults currents on dc traction supply," *IET Power Electronics*, vol. 1, no. 3, pp. 348–355, 2008.

[8] P. Pozzobon, "Transient and steady-state short-circuit currents in rectifiers for dc traction supply," *Vehicular Technology, IEEE Transactions on*, vol. 47, no. 4, pp. 1390–1404, 1998.

[9] M. Berger, C. Lavertu, I. Kocar, and J. Mahseredjian, "Performance analysis of dc primary power protection in railway cars using a transient analysis tool," in *Vehicle Power and Propulsion Conference (VPPC), 2015 IEEE*. IEEE, 2015, pp. 1–7.

[10] J. Brown, J. Allan, and B. Mellitt, "Calculation of remote short circuit fault currents for dc railways," in *IEE Proceedings B (Electric Power Applications)*, vol. 139, no. 4. IET, 1992, pp. 289–294.